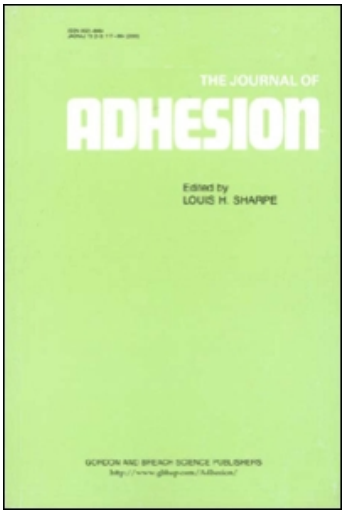

The Journal of Adhesion

Publication details, including instructions for authors and subscription information:
http://www.informaworld.com/smpp/title~content=t713453635

Interactions Between Micron-sized Glass Particles and Poly(dimethyl siloxane) in the Absence and Presence of Applied Load

Gary Toikka[a]; Geoffrey M. Spinks[a]; Hugh R. Brown[a]
[a] Institute for Steel Processing and Products, University of Wollongong, NSW, Australia

To cite this Article Toikka, Gary , Spinks, Geoffrey M. and Brown, Hugh R.(2000) 'Interactions Between Micron-sized Glass Particles and Poly(dimethyl siloxane) in the Absence and Presence of Applied Load', The Journal of Adhesion, 74: 1, 317 — 340
To link to this Article: DOI: 10.1080/00218460008034534
URL: http://dx.doi.org/10.1080/00218460008034534

J. Adhesion, 2000, Vol. 74, pp. 317–340
Reprints available directly from the publisher
Photocopying permitted by license only

Interactions Between Micron-sized Glass Particles and Poly(dimethyl siloxane) in the Absence and Presence of Applied Load*

GARY TOIKKA†, GEOFFREY M. SPINKS and HUGH R. BROWN

Institute for Steel Processing and Products, University of Wollongong, NSW 2522, Australia

(Received 15 June 1999; In final form 15 November 1999)

A technique using a scanning electron microscope to view a fine particle in contact with a flat substrate whilst under load and during its removal is described. The particle is attached to an atomic force microscope cantilever so that the magnitude of the load can be estimated directly from the imaged deflection. Interactions between 5 to 60 μm spherical glass particles and cross-linked poly(dimethyl siloxane) were studied in the presence and absence of load. W_A was estimated to be 74 mJ/m^2 from the size of the contact area in the absence of load. Using highly flexible cantilevers to apply load resulted in large shear displacements and forces, which distorted the contact area and assisted in particle removal. These shear effects were eliminated by using a more rigid cantilever to measure a normal pull-off force for which the interface toughness, G_c, exceeded 950 mJ/m^2. The large adhesion hysteresis indicated the presence of chemical bonding, presumed to occur between silanol and siloxane groups. The mode of particle detachment varied significantly with the choice of cantilever, showing evidence of both cohesive failure and interfacial crack propagation. The relevance of these results to the interpretation of AFM data is discussed.

Keywords: Particle removal; Applied load; Shear; Elastic JKR deformation; Glass particles; Poly(dimethyl siloxane)

* Presented in part at the 22nd Annual Meeting of The Adhesion Society, Inc., Panama City Beach, Florida, USA, February 21–24, 1999.

†Corresponding author. e-mail: gtoikka@uow.edu.au

INTRODUCTION

Significant effort has been expended on the study of fine particle interactions, largely due to their importance in technological processes ranging from mineral flotation to photocopying. In most of these processes the particles make *contact* with dissimilar surfaces, hence, the magnitude of the adhesion or, most importantly, the ease of their removal becomes of considerable practical interest. As the adhesion is controlled by processes that occur within the contact area, both the contact mechanics and the interfacial properties must be given consideration. Given the small size of the particles and the magnitude of the forces involved, highly specific techniques are required to study the adhesion directly.

The development of the atomic force microscope (AFM) has permitted forces less than 10^{-11} N to be directly measured between imaging tips [1, 2] and flat surfaces. Unfortunately, since the tips are only nm in size and difficult to characterise [3] the data obtained are not directly useful for understanding fine particle adhesion. The problem has been resolved by attaching micron [4] and sub-micron [5] sized particles to AFM imaging tips to measure forces against both flat [6, 7] and spherical substrates [8, 9]. Studies focussed on the measurement of adhesion [10 – 12] have given values distinctly less than that expected on a theoretical basis. The findings were rationalised in terms of surface roughness where asperities increased the effective separation to reduce the intimate contact area. The explanation coincides well with increases in the adhesion using deformable surfaces and stiff cantilevers [13], as load more readily places the particles in intimate contact. However, a number of effects inherent in the normal operation of the AFM limit its use as a dedicated adhesion-measuring device.

AFM's are unable to hold a single contact between a particle and substrate over an extended time period. Since adhesion often increases with time, the measured values are likely to be poor indicators in most real applications. Several contacts are also made over relatively short time periods, which has the potential to deform the substrates and to make the overall interaction geometry ill-defined. The measured forces are assumed to be normal to the plane of the interaction, following the use of a laser and split photodiodes to detect cantilever deflections. Whilst the assumption is reasonable as the particle approaches the

substrate, the very geometry of the technique makes shear forces at contact inevitable. As the extent of shear forces in AFM experiments is difficult to know, the interpretation of contact data is somewhat unclear.

Scanning electron microscopes (SEM) have also been used to study the adhesion between micron-sized particles and flat substrates [14–19]. The technique has enabled particles in extended contact with flat substrates to be viewed directly. It was found that significant deformation occurred in the contact area, which, in instances, allowed the adhesion to be indirectly determined. The values were normally an order or more greater in magnitude than those measured using an AFM. It is reasonable that longer contact times lead to increases in the measured adhesion as more intimate contact forms. Further increases in the measured adhesion can also be expected when removing particles from SEM experiments as separation processes include hysteresis mechanisms [20].

Whilst the detachment of a particle from a surface is ultimately governed by the magnitude of the adhesion, the efficiency of a removal processes may also depend on shear forces. For instance, the use of hydrodynamic flow to clean silicon wafers is based on drag and lift forces, for which the latter may be negligible inside the boundary layer. Smaller particles must then be dislodged at an angle to the interaction plane until the adhesion is overcome [21]. Quantitative differences in the magnitude of the normal and shear force required to remove micron-sized particles have been directly measured using an atomic force microscope [22]. It was found that removal was more easily facilitated by shear forces than lift (pull-off) forces for interactions between rigid surfaces. The relationship between the two forces may change if deformable substrates are used, as the particles can be displaced into the surface. One of the aims of this work is to examine explicitly the effects of shear forces on adhesion measurements and particle removal.

JKR [23] adhesion theory predicts a relationship between the thermodynamic work of adhesion W_A [24] and the elastic deformation of macroscopic bodies in contact. The features between an ideal rigid spherical particle and a flat deformable surface are illustrated in Figure 1. As the model is based on an energy balance, it neglects any surface forces outside the contact zone to predict, unrealistically,

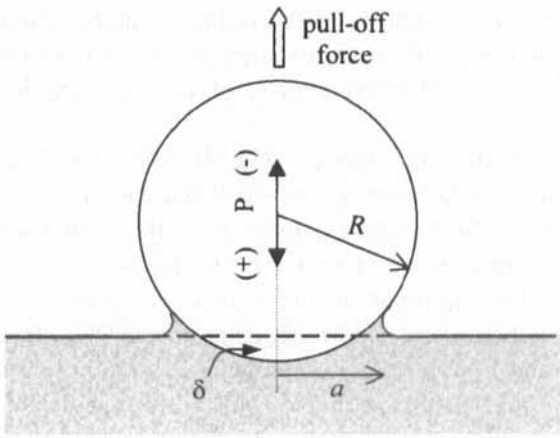

FIGURE 1 Contact size (radius, a) and shape between an elastically deformed flat surface and a particle (radius R). The central axis (dotted line) is indicated, along which displacement (δ), normal load (P) and pull-off force are determined.

infinite tensile stresses at the contact edge. The presence of the tensile forces in the outer contact region result in the distinctive non-Hertzian contact shape described as a "neck". The size of the contact radius, a, is given by

$$a^3 = \frac{R}{K}\left\{P + 3W_A\pi R + \left[6W_A\pi RP + (3W_A\pi R)^2\right]^{1/2}\right\} \qquad (1)$$

where R is the particle radius, K is related to the elastic modulus, E, and Poisson ratio, ν, of the materials and P is the normal applied load. It should be noted that, by convention, a compressive (tensile) load is positive (negative) and expected to increase (decrease) the contact radius. For the contact radius to decrease in size, a crack must propagate along the interface between the two materials and Eq. (1) can be considered in terms of fracture mechanics. Whilst crack growth is typically not an equilibrium process, the equation remains valid as long as the strain energy release rate, G, is substituted for W_A. Sufficient reduction in the load causes crack propagation to occur when G reaches its critical value, G_c, which itself may depend on crack propagation rate. In this paper we shall consider crack propagation in terms of G_c and the reverse, contact growth, as an approximate

measure of W_A. The difference between the values of G_c and W_A obtained in this way is often referred to as "adhesion hysteresis".

The adhesion also places the central contact region under compressive stress, even in the absence of external load, displacing the particle into deformable surfaces along the central axis by δ [25]

$$\delta = \frac{a^2}{3R} + \frac{2P}{3aK} \tag{2}$$

Hence the displacement, as in the case of the contact radius, can be expected to increase with compressive load. It is possible to displace the particle in a negative direction above the interaction plane to cause stable crack propagation, which reduces the contact patch until a finite size of the crack becomes unstable and separation occurs. The negative normal load at this instant is known as the pull-off force and is directly related to G_c *via*

$$F_p = \frac{3}{2} G_c \pi R \tag{3}$$

In the absence of any load, Eq. (1) is reduced so that a linear relationship between the contact radius and the particle radius to the power 2/3 can be expected. The relationship has been independently verified for mm-sized rubber hemi-spheres [23] using optics to view the contact directly. It has also been observed between micron-sized glass particles and polyurethane [15, 26] using a SEM. The findings confirmed the extension of current elastic deformation theory to particles $> 5\,\mu m$ in the absence of load. An extremely useful feature of the approach is that values for W_A may be experimentally determined. These values are able to include many of the non-idealities, such as surface contamination or roughness, which are typically encountered in real systems but are not amenable to theoretical analysis.

This paper describes a novel technique to view and directly measure fine particle adhesion, based on the principles of both an AFM and a SEM. The technique has been used to study interactions between spherical micron-sized glass particles and flat polydimethylsiloxane (PDMS) surfaces. This model system was chosen because (a) PDMS is known to deform mainly in an elastic manner with little viscoelastic effects, (b) it is possible to measure glass-PDMS adhesion on a much

larger size scale using a JKR apparatus, and (c) the adhesion between PDMS and silicon oxide shows interesting effects that have been ascribed to hydrogen bonding between silanol groups and the siloxane groups of the PDMS [27]. These effects have been seen in studies of the adhesion of PDMS to the oxide surface of a silicon wafer and the adhesion of a plasma-oxidised PDMS surface to an unoxidised surface. It would not be unreasonable to expect similar adhesion mechanisms between oxidised glass surfaces and PDMS. If contact is formed over longer time period, significant increases in the adhesion may also occur due to surface reconstruction reactions, as has been seen with hydrolysed PDMS surfaces [27–29].

EXPERIMENTAL

Spherical 5–60 μm glass particles were obtained from Duke Scientific (California, USA) and used without further treatment. PDMS sheets were prepared by using 0.0542 g of methylhydrosiloxane to cross-link 1.5087 g of vinyl-terminated, 9600 molecular weight poly (dimethylsiloxane) in the presence of ~8 ppm platinum-divinyl-1-tetramethyldisiloxane complex used as catalyst (Gelest, Inc). A 68% stoichiometric excess of cross-linker was used to ensure that a fully-reacted elastomer network was produced. Both flat and (~1 mm) hemispherical substrates were made and cured in air at 75°C for 2 hours. The elastic modulus (E) of the PDMS, 0.91 MPa, was determined using a JKR set-up to measure symmetrical interactions (self-adhesion) between the two geometrically different substrates. The flat PDMS samples were also cut into approximately $1 \times 1\,cm^2$ pieces and placed on SEM stubs and the force rig (see below) sample holder. The glass particles were either sprinkled onto the PDMS from heights less than 1 cm, or placed directly into contact using a micro-manipulator or AFM cantilevers. All interactions were kept at 20°C for 7 days prior to imaging to allow (near) equilibrium conditions to be reached. The particle surfaces were also imaged using an atomic force microscope (Digital Instruments, Inc.) to reveal an average RMS surface roughness of 2.7 ± 0.4 nm over select $1 \times 1\,\mu m^2$ areas. Significantly rougher regions, which were more readily observed using light microscopy and SEM, could also be detected. Overall, the glass was considered rough

on both microscopic and macroscopic scales. The PDMS appeared smooth in SEM observations and was not explored further as significant deformation of the surfaces were expected.

All SEM images were measured using a secondary-electron emission electron microscope (Leica 440 Stereoscan). The tungsten filament was operated at 20 kV whilst varying the probe current between 100 – 300 pA to obtain best resolution. Due to the low conductivity of PDMS and glass all samples were sputter coated (Dynavac Magnetron, SC100MS) with platinum immediately prior to being imaged, to avoid artefacts due to either charging or Joule heating. To ensure the platinum thickness was insignificant in the measurement of contact radii, it was kept to approximately 6 nm by sputtering for 30 seconds at 50 mA (~ 2 Å/sec), as determined using a quartz microbalance. All images were measured at $< 2°$ off the interaction plane to best observe the contact regions. At such small angles, care was required to avoid any foreground roughness which may have prevented the contact areas from being directly viewed.

The force rig (Fig. 2a) was designed to allow an AFM cantilever to be manipulated with sub-micron resolution whilst inside a SEM chamber. A high-precision sliding rail (Del-Tron) was used to move

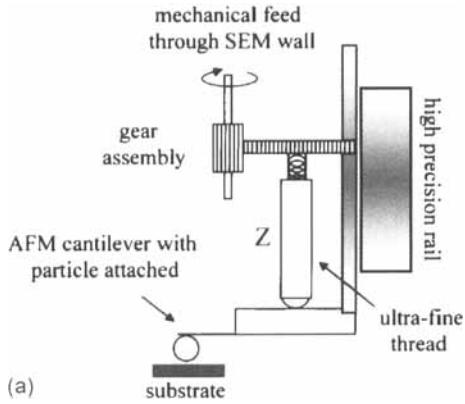

FIGURE 2 (a) Schematic of the force rig designed to apply loads to micron-sized particles whilst inside a SEM, described in text. (b) SEM micrograph of interactions between glass particles, in the size range of 3.3 – 20 μm (radius), and cross-linked PDMS. The particle on the right can be seen under the load of an AFM cantilever and the other five in the absence of applied load.

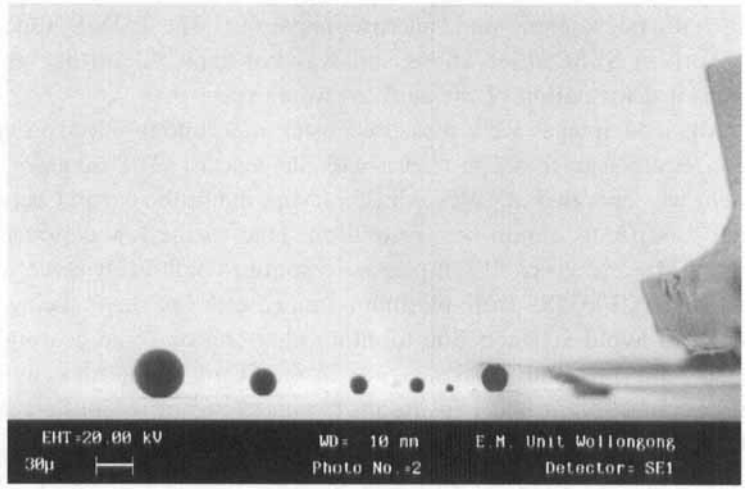

(b)

FIGURE 2 (Continued).

the cantilever in a z-direction (normal) to the sample. Their separation was controlled using an ultra-fine thread (Newport) and mechanical gearing. A locking screw was used to ensure that no changes occurred in the z-displacement whilst fitting the force rig into the SEM chamber. It also enabled the contact made between the glass particles and the PDMS under a light microscope to be maintained for 7 days before imaging in the SEM. The integrity of the rail and the complete force rig was tested as follows for run-out or "glitch". A polished tin/lead alloy flat was indented using a stiff (tapping mode) cantilever and its relative position imaged as the load and separation was altered. Out of contact, less than 0.2 µm lateral movement in the image plane, perpendicular to the z-direction, could be detected. To operate the force rig externally to the SEM a mechanical feed-through was installed in the microscope vacuum chamber door. An infrared viewing camera (Robinson Chamber View) was fitted inside the vacuum chamber to ensure that no contact was made between the (approximately 100 mm long) force rig and the SEM interior.

The glass particles were attached to highly-flexible, triangular-shaped (contact mode) and rigid-beam-shaped (tapping mode) AFM cantilevers (Digital Instruments, California), using a technique described elsewhere [11]. The stiffness of the cantilevers was determined from measurements of their resonance frequencies, in the

absence and presence of a known mass. Hooke's law was used to evaluate the load on the particles once the deflection of the cantilever, away from its zero-force position, was estimated from the SEM images. Interactions between several glass particles and PDMS can be seen on the sample holder of the SEM force rig in Figure 2b. The particle on the right is under the load of an AFM cantilever, whilst the other (five) particles were kept in the absence of applied load. Their inclusion enabled confidence to be gained that there was no significant variation in the conditions between experiments. Note that the individual legs of the triangular-shaped cantilever can barely be discerned to confirm that the interactions were imaged close to the interaction plane.

RESULTS AND DISCUSSION

Interactions between glass particles and PDMS were studied after seven days in contact in (a) the absence of any load, (b) in the presence of small loads applied using highly flexible cantilevers and (c) large loads applied using stiff cantilevers. In the absence of load the contact between a 10.9 μm glass particle and PDMS (Fig. 3) was found to be significantly larger than one would expect between two totally rigid surfaces. The contact shape was clearly non-Hertzian, providing evidence of tensile forces in the outer region of the contact. As the interaction occurred in the absence of any load the deformation of the PDMS was solely attributed to surface forces. Note that the elastic modulus of the PDMS is almost five orders of magnitude less than that of glass, hence any deformation of the latter has not been considered in this study. The contact radius between several particles and PDMS were measured and plotted (Fig. 4), in log form, against the particle radius to find if the deformation was indeed elastic. A linear regression revealed a 0.66 power law dependence between the respective radii, which is in excellent agreement with the JKR elastic deformation theory of Eq. (1). The measurement of contact between a wide range of rigid small particles and deformable surfaces (or *vice versa*) has revealed similar power laws to that observed here and also at 0.42 [17] and 0.75 [30]. It was, of course, expected that a cross-linked polymer, such as the PDMS used here, would behave in an elastic manner well above its glass transition temperature (−123°C). The large

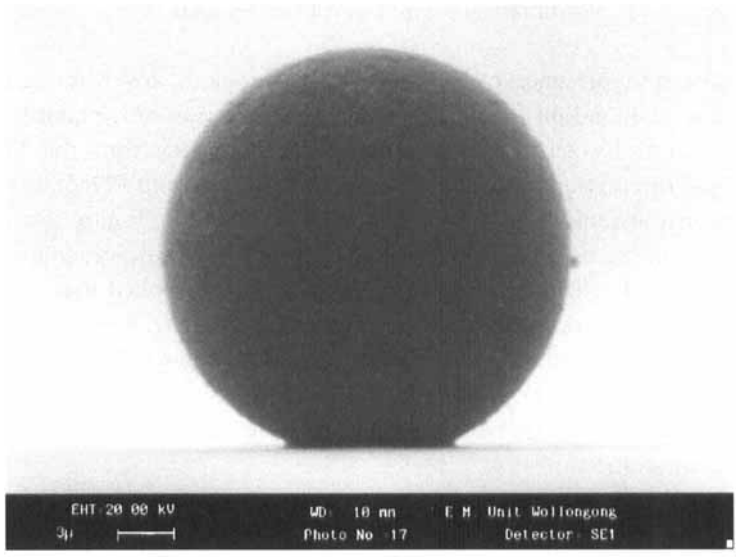

FIGURE 3 A 10.9 μm radius glass particle kept in contact with PDMS for 7 days, in the absence of applied load. The formation of a "neck" is clearly visible and has been predicted by JKR [23] theory.

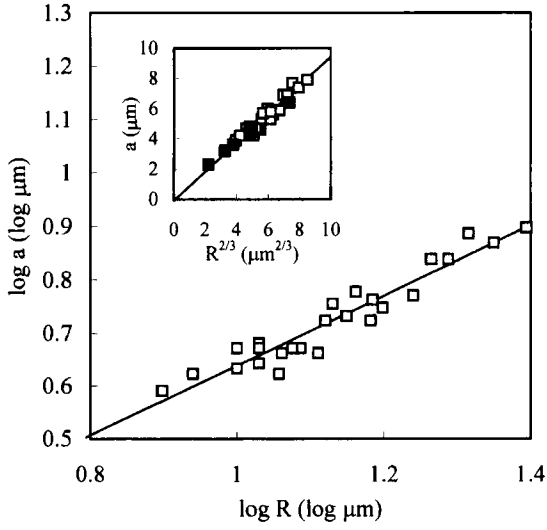

FIGURE 4 Log plot of contact radius, a, as a function particle radius, R, between glass particles and PDMS in the absence of external load. A linear line of best fit, $a = 0.66R - 0.02$ (Rsq, 0.91), is indicated. The plot of a as a function of $R^{2/3}$ (inset) results in a slope of 0.0095 and an intercept of 0.0773 (μm). Data (black squares) from the particles in Figure 2b have been included.

experimental scatter (Rsq. 0.91), also observed elsewhere, was most likely due to the excessive macroscopic scale roughness of the glass particles.

Having established the nature of the deformation, the value of G, $74\,mJ/m^2$, was readily obtained from the slope of the contact radius as a function of the particle radius to the power 2/3 (Fig. 4, inset). Interactions between larger PDMS elastomers in (~ 30 minutes) contact with glass slides were also measured to yield significantly lower values, between $44-47\,mJ/m^2$, for G. The reason for the increased adhesion in the smaller interactions is not known but may simply have arisen from the longer contact times (both systems are currently the subject of further study). Under the experimental conditions, the value of G (for contact growth) is assumed to have reached equilibrium and has, for the purpose of this study, been equated to W_A. The zero (within experimental error) intercept confirmed the assumption of no external forces having contributed to the deformation. In the event of the adhesion having occurred solely as a result of dispersion forces, the interfacial energy of each respective surface can be related through the approximation [31] $W_{A(glass/PDMS)} \approx 2(\gamma_{glass}\gamma_{PDMS})^{1/2}$. The interfacial energy of the PDMS surface, $\gamma_{PDMS} = 23.4\,mJ/m^2$, was measured in self-adhesion measurements and implies a value of $57.8\,mJ/m^2$ for the glass surface. Whilst glass is a high energy surface [31] the low value obtained here is reasonable as the particles were most likely covered with adventitious hydrocarbons prior to making their contact with the PDMS. Neither the measured nor derived value confirms (or discounts) the origin of the adhesion between the glass and the PDMS. The W_A reported here lies well within the broad boundaries of 44 [30] and 120 [26] mJ/m^2 previously determined between polyurethane elastomers and micron-sized glass particles.

The contact between the ($10.5\,\mu m$) glass particle and PDMS under compressive load in Figure 2b can be seen at a higher magnification in Figure 5. A highly flexible cantilever (stiffness, $0.029\,N/m$) was used to apply the small load, estimated to be $0.80 \pm 0.03\,\mu N$ in magnitude. The $10.9\,\mu m$ glass particle in the absence of load shown in Figure 3 was also from the same experiment (second from the left in Fig. 2b). Given that both particles were kept under identical experimental conditions and are similar in size, the effect of load on the contact could be determined unequivocally. On closer inspection, it is evident that

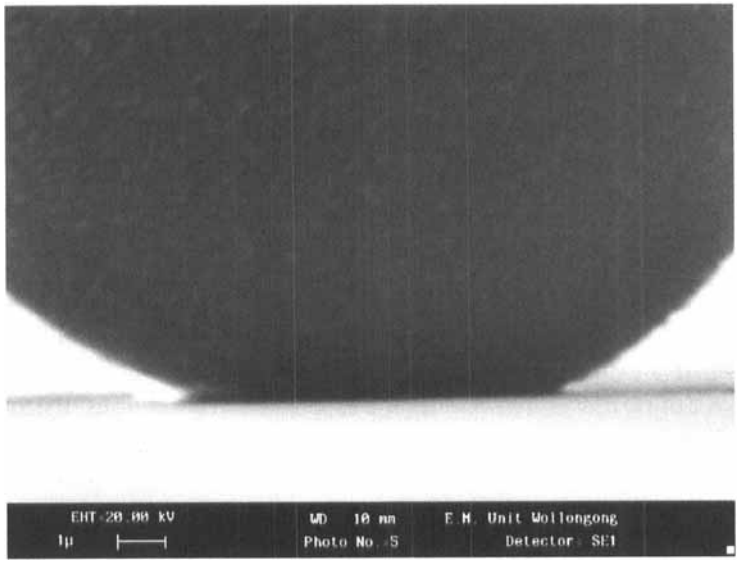

FIGURE 5 Contact area between the 10.5 μm glass particle observed under load in Figure 2 and PDMS. Its contact patch can be unequivocally compared with the particle in Figure 3 as both particles were kept in contact with the same PDMS and are virtually identical in size.

the particle under load is displaced further into the PDMS and the surrounding contact region is somewhat displaced. Under the conditions, the central displacement was expected to increase from 0.67 μm to 0.78 μm with the load, and whilst an increase could be confirmed, the respective measured values of 0.45 ± 0.05 μm and 0.70 ± 0.05 μm were both smaller than predicted. It was also anticipated that the contact radius would increase from the measured 4.67 ± 0.1 μm to the predicted 4.85 μm with the load; surprisingly, it was found to have been reduced to 3.95 ± 0.1 μm. The observation can be rationalised in terms of shear forces, which arise from using the highly flexible cantilever to apply the load. The initially straight AFM cantilever can be seen, in Figure 2, to bend into an arc as contact is made between the particle and the PDMS. Considering that the cantilever approached the interaction plane at approximately 12°, in a similar set-up to that used in an AFM, shear forces from both slip and rotation of the particle are likely to arise. Barquins [32] observed similar reductions in the contact between mm-sized glass hemi-spheres

and flat rubber surfaces whilst studying the effect of shear forces. He discovered that the contact shape became asymmetric as it was reduced in size. Once the glass began to slip, the rubber immediately surrounding the contact was also displaced in an asymmetric manner. There is evidence of both these effects in the contact and immediate surroundings of the PDMS and the glass particle in Figure 5. Unfortunately, the contrast resolution of the SEM and the physical impossibility of imaging a profile at 0° to the interaction plane prevented a more quantitative comparison from being made. It was also not possible to unequivocally determine the nature of the contact shape under load as only one (left) side can be discerned as non-Hertzian.

The load on the glass particle in Figure 5 was gradually decreased until a tensile force was applied (Fig. 6a). It can be seen that the cantilever bends away from the PDMS surface near its fixed end, and towards the PDMS surface closer to the particle contact area. The observed S-shape shows that the mechanical action of the AFM

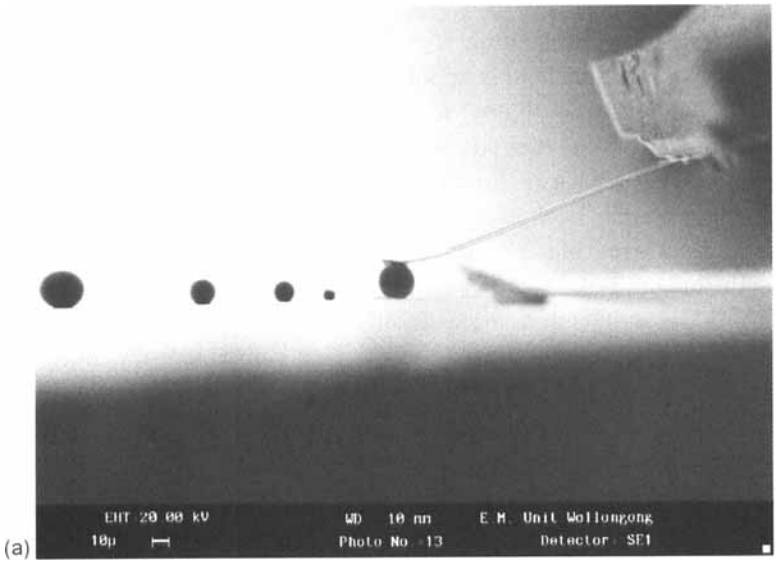

(a)

FIGURE 6 (a) Tensile load applied to the glass particle observed in Figure 5 can be seen to result in an S-shape bend of the highly flexible (stiffness, 0.029 N/m) AFM cantilever, which (b), distorts the PDMS in a manner clearly not normal to the plane of interaction.

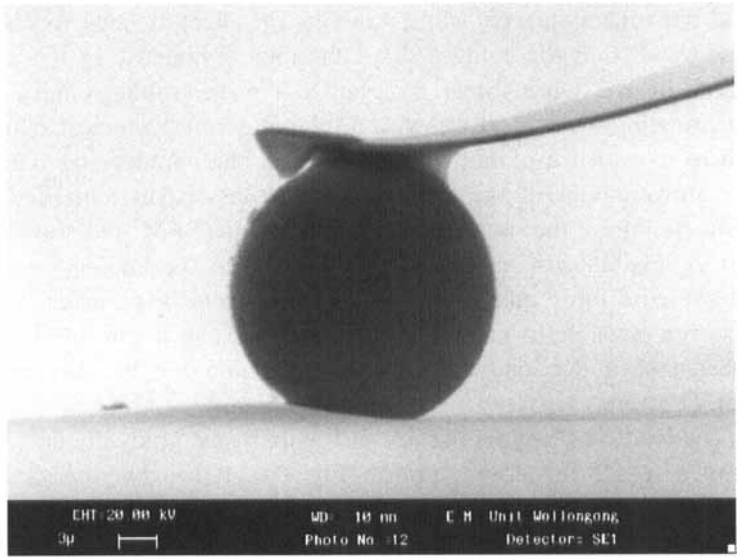

(b)

FIGURE 6 (Continued).

cantilever during unloading is not simply the reverse action to that when a compressive load is applied. Under the negative load there are clearly two forces on the particle, in addition to that applied in the z-direction: a torsion created by the bend in the cantilever and a pull towards the force rig as the cantilever struggles to span the distance to the contact area. Both effects inevitably contribute to shear forces in the contact area but it is difficult to know their magnitude. Some insight into the overall force acting on the particle can be gained by viewing the contact area more closely (Fig. 6b). The PDMS is severely distorted in an asymmetric manner which confirms that the total force applied on the glass particle is not normal to the interaction plane. Evidence of the torsion can also be seen in the relative position of the glass particle to the AFM imaging tip in Figures 2b and 6. As load is applied to the cantilever, the two-part epoxy glue deforms and allows the particle to move closer to the imaging tip. This observation confirms the need for careful selection of the adhesives used to attach particles to AFM cantilevers. Incidentally, if one monitored the deflection of the cantilever in Figure 6 using only a laser reflected off the tip, it would be difficult to avoid the conclusion that the particle

was, in fact, under a positively applied load. Hence, in an AFM experiment it would be hard to distinguish the current situation from that observed in Figure 2. It is interesting to note that in the presence of shear, the size of the particle contact radius was larger under the tensile load ($4.77 \pm 0.1\,\mu m$) than under the compressive load ($3.95 \pm 0.1\,\mu m$).

To determine the value of G_c required to propagate a crack which leads to the removal of a glass particle from the PDMS, a pull-off force normal to the plane of interaction must be applied until separation occurs (Eq. (3)). This condition is often assumed in the use of cantilever-based techniques, such as the AFM. From the previous discussion it is clear that a flexible cantilever, such as the one used here, cannot directly measure G_c. There is, however, the prospect that the mechanics of the cantilever could be analysed, prior to detachment, in order to gain an understanding of the forces acting on the particle. This approach could prove useful in the analysis of real processes where both shear and normal forces are inevitable during detachment. Figure 7 shows the glass particle viewed in Figure 6,

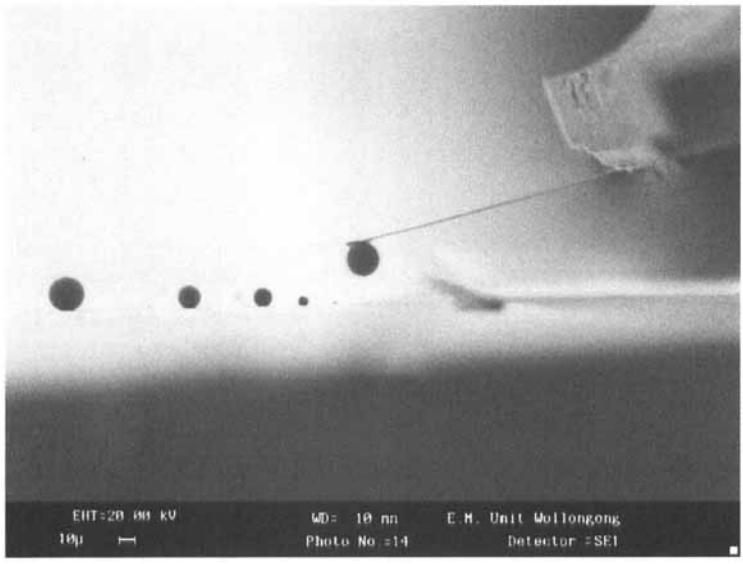

FIGURE 7 Displacement between the glass particle in Figure 6 and PDMS immediately following detachment. The straightness of the cantilever confirms that no permanent bends resulted from it being placed under load.

immediately following its detachment from the PDMS surface. Unfortunately, it was not possible to obtain images of the actual detachment process, as it occurred over a very short (less than 1 second) time period. The linearity of the cantilever in the absence of load confirms that it was not permanently deformed and validates the assumption of the zero-force position used in the estimate of load. The (z) displacement between the particle and the PDMS corresponds to a "normal" pull-off force equivalent to a G_c value of $10.6\,mJ/m^2$.

Figure 8 shows the detached glass particle and the PDMS imaged at 10° above the interaction plane. Substantial deformation of the PDMS can be seen from this angle and can be readily attributed to cohesive failure since a large piece of the elastomer is also visible on the glass particle. Had the experimental conditions been such that the particle could not be viewed after it was removed, the deformation may well have (in less elastic systems) been mistaken as being plastic in nature. Since the PDMS piece on the glass particle is smaller in size ($\sim 4\,\mu m$) than the contact area was prior to detachment, the mechanism for particle removal in the presence of shear forces

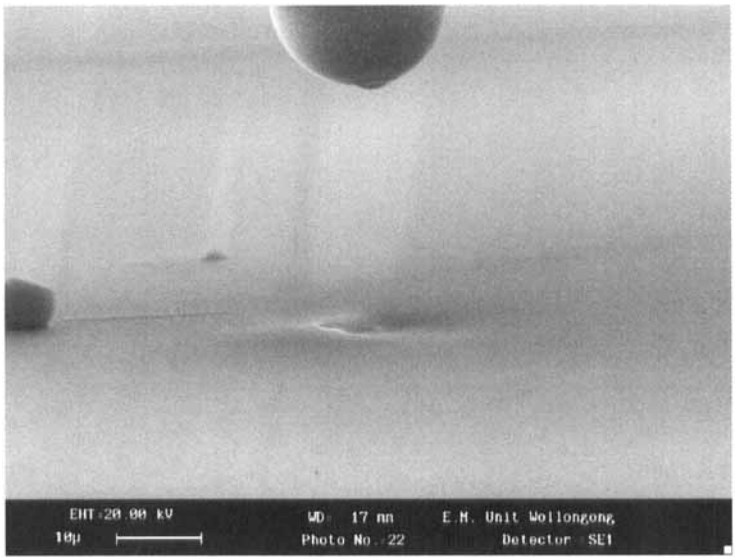

FIGURE 8 A close-up of the glass particle and PDMS in Figure 7 imaged at 10° to the interaction plane. Cohesive failure of the PDMS is evident as a large piece of the elastomer remains attached to the glass particle.

was through a reduction in the contact radius until cohesive failure occurred. Several more experiments were conducted using highly-flexible cantilevers to determine if the cohesive failure could be eliminated. It was found that by using small increments of load, the particles could be detached without any visible signs of PDMS on them. In these instances, an equivalent normal G_c up to 43 mJ/m^2 could be measured; however, in none of the experiments were we able to obtain a value for $G_c > W_A$. Even under the most ideal conditions, the value of G_c must exceed its equilibrium adhesion value, W_A, otherwise detachment could not occur. The result obtained here clearly demonstrates the importance of shear forces in particle removal. It also explicitly shows why an AFM cannot measure strong adhesion using a highly flexible cantilever.

To minimise the effect of shear, a cantilever with a stiffness of 42.7 N/m was used to place a 12.8 μm glass particle (Fig. 9) under positive load against PDMS. The inclusion of a zero-force line (arrow) reveals that the deflection could easily be resolved at a load of 57 ± 11 μN, although the precision was significantly less than when

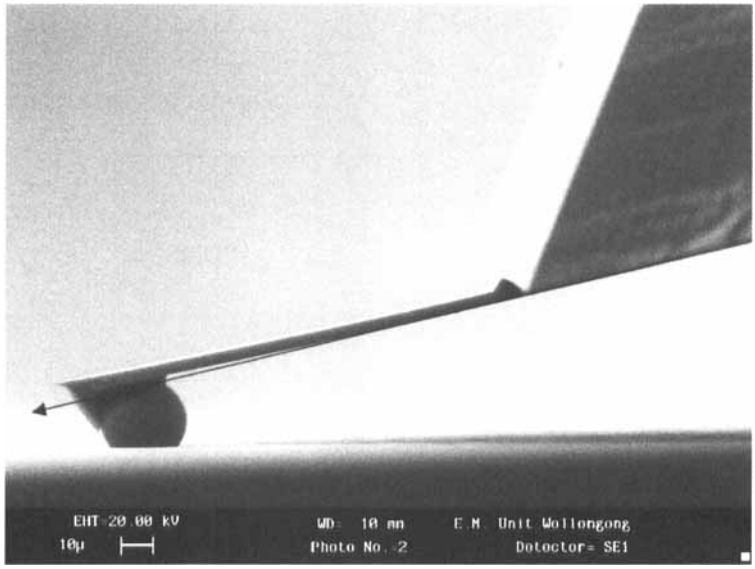

FIGURE 9 Compressive load applied to a 12.8 μm glass particle in contact with PDMS using a stiff (42.7 N/m) AFM cantilever. The arrow illustrates the small deflection required to apply a load which significantly deforms the PDMS.

using the more flexible cantilevers. The actual contact between the particle and the PDMS cannot be directly viewed as the particle is displaced well into the PDMS surface. Its expected [33] profile is illustrated in Figure 10 which predicts the contact radius to be 9.2 μm and the central displacement 4.8 μm, under the estimated load. The measured displacement, 4.8 ± 0.2 μm, coincides well with theory to suggest that the deformation had remained elastic in nature. In order to inspect the contact, the load on the particle was reduced to approximately zero and imaged (Fig. 11a) immediately afterwards. The size of the contact radius, 9.0 ± 0.2, was (within experimental error) the same as that predicted prior to having reduced the load. This suggested that little, if any, change had occurred in the contact region during the process. Hence, the clearly visible "neck" was assumed to have formed under compressive load and has only previously been observed between larger (mm) sized substrates. The interaction profile in Figure 10 does not explicitly accommodate spherical particles (as it is based on a parabola) and lacks in continuity immediately next to the

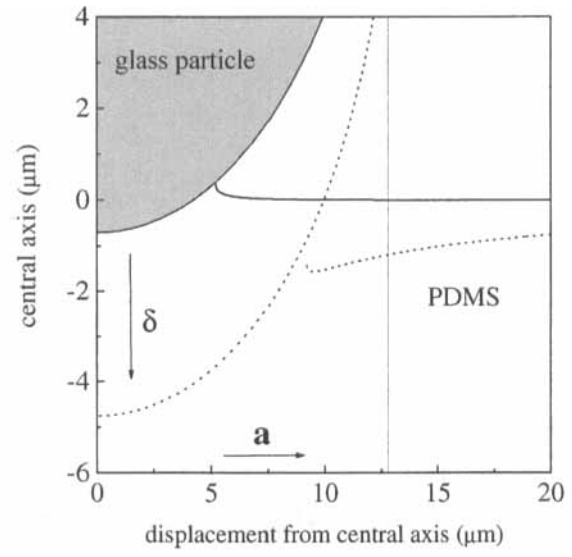

FIGURE 10 Predicted [32] interaction profile of PDMS under zero (solid line) and 57 μN load (dashed line) of a 12.8 μm glass particle. The values used in the calculations were W_A, 74 mJ/m^2, E, 0.91 MPa; ν, 0.5 and E, 70 GPa; ν, 0.3 for the respective surfaces. Increases in the contact radius, a, and the central displacement, δ, are expected with load.

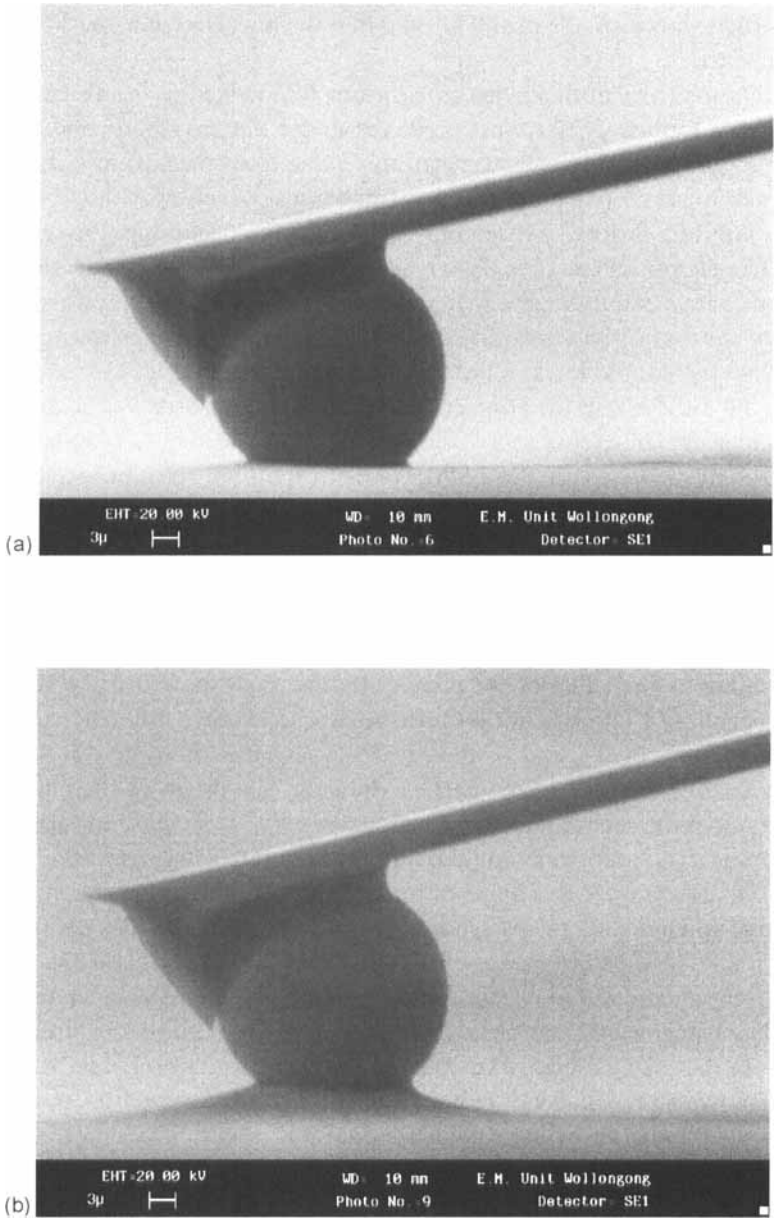

FIGURE 11 (a) Contact between the glass particle and PDMS observed in Figure 9 immediately after the applied load was reduced to (approximately) zero and (b) later under a load of $(-)57 \pm 11\ \mu N$.

particle; however, it can still be seen that the non-Hertzian "neck" was expected.

On the basis of the (near) equilibrium W_A derived in the absence of load, a radius of 5.20 μm is predicted under the zero load conditions in Figure 11a. However, to reach this value from the 9.0 μm radius, a crack must propagate between the materials. Crack growth is *not* an equilibrium process and can only be expected to occur once the critical strain energy release rate, G_c, is reached. Since there was no reduction in the contact radius at zero load, even after several minutes, it was soon evident that G_c was greater in magnitude than W_A for the system. The load was reduced to a tensile force of $(-)\ 57 \pm 11$ μN (Fig. 11b) where a small reduction in the contact radius, 8.7 ± 0.2 μm, could be detected. Under the large tensile force the particle can be seen to have remained strongly attached to the PDMS, which deforms well above the interaction plane. The particle is, in fact, negatively displaced at $(-)\ 1.2 \pm 0.13$ μm above the (flat) PDMS surface. At this point, which represents the final load increment prior to detaching the particle, a conservative value was estimated for G_c (from the load and the displacement) at $950 \pm 180\ \text{mJ/m}^2$. It should be noted that under these conditions the value of the contact radius was expected to be slightly smaller (8.1 μm) than that measured. The massive difference in the magnitudes of W_A and G_c indicates a large adhesion hysteresis which makes the removal of the particle difficult. The origin of the increased adhesion cannot simply be rationalised by an increase in intimate contact with load, as it would require the interfacial energy of the glass from dispersion forces alone to be $9.6\ \text{J/m}^2$. The value is unrealistically large and indicates the presence of chemical bonds, most likely between silanol and siloxane groups of the glass and PDMS surfaces [27].

The interaction between a glass particle and PDMS under tensile load using a stiff cantilever in Figure 11b is remarkably different from that using a highly-flexible cantilever (*cf.* Fig. 6b). It can be seen that whilst the particle remains in contact the interaction is close to symmetric, providing evidence that the shear forces have been minimised. There remains, however, a small element of asymmetry as the bend in the cantilever causes the particle to "lean" slightly to the right. On closer inspection, small differences between the left and right hand side profiles can also be discerned, which, in essence, must have different values of G_c. It would, therefore, be unreasonable to expect detachment to occur *via* a symmetric reduction in the contact radius

until instability is reached at a given load. Figure 12 shows an instant in the actual detachment process of the glass particle from the PDMS to confirm the supposition. A crack can be seen to propagate from the left side of the particle as the right side remains firmly in contact, the process occurring over several 10's of seconds. The mechanism for particle removal under minimal shear force was through a small reduction in the contact radius until a more rapid crack propagated from one side. There was no visible evidence of cohesive failure of the PDMS, unlike when removal occurred in the presence of strong shear forces. Once the glass particle was detached, the PDMS returned to its flat geometry within a few seconds with a minimal amount of residual build-up (of unknown origin) surrounding the contact patch. Whilst the work presented here has been concerned with the study of fine particle interactions, its significance to AFM use warrants a short summary. It has been illustrated that both the adhesion and the applied load, between a probe and a sample, result in cantilever distortions which give rise to non-normal forces. Whilst higher applied loads and higher adhesion forces than those usually encountered in

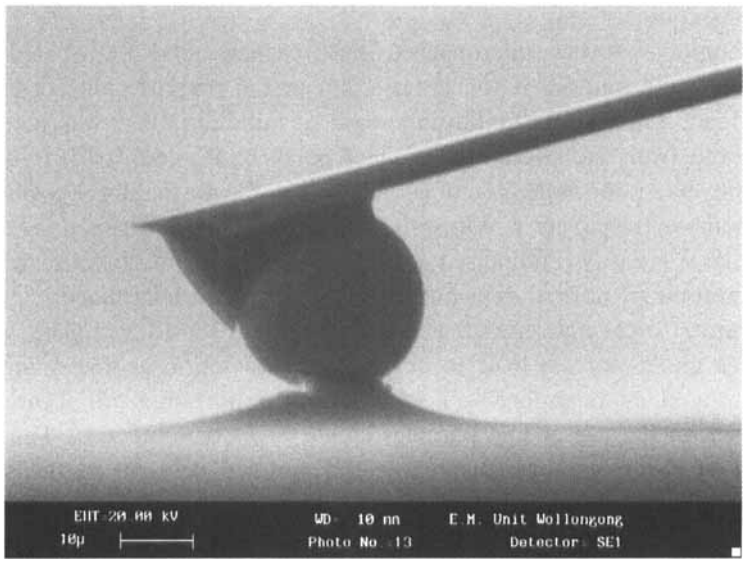

FIGURE 12 Detachment of the glass particle observed in Figure 11 from the PDMS surface can be seen to occur *via* the propagation of a crack on the (left) side farthest away from the fixed end of the cantilever.

AFM measurements have been studied here, there is little reason to suspect that the relative contribution of non-normal forces under small loads or weak adhesion would be less significant. Attard [34] has calculated that applying loads as small as 5 nN on an imaging tip in contact with a flat sample causes hysteresis in the constant compliance region due to shear caused by friction. Since cantilever distortions are difficult to characterise or even to detect in an AFM, the contribution of shear forces to measured data cannot be unequivocally determined. It has also been shown here that the role of compliant materials, used for particle attachment and surface modifications, must be given serious consideration.

CONCLUSIONS

A new technique has been used to study interactions between micron-sized particles and flat substrates under applied load. Its advantages include the ability to examine contact mechanics in the smaller particle size domain, to measure directly and to observe particle removal under variable shear forces and to provide insight into the interpretation of AFM contact data.

Contact between micron-sized glass particles and PDMS led to elastic deformation of the latter, both in the presence and absence of load. The (near) equilibrium work of adhesion, W_A, was readily derived from the size of the contact patch under zero load. It was, however, a poor indication of G_c and, hence, the normal force required to remove the particles. Whilst the large disagreement between the two values was easily rationalised, it highlights the need for direct removal of particles if normal detachment forces are to be determined.

Shear forces deformed the contact between PDMS and glass particles under normal load to change the interaction geometry significantly. Understanding such changes are important to applications based on the use of fine particles as abrasives or lubricants. The effect of shear was also distinct in the removal of glass particles as it was able to reduce the measure of G_c and even to change the mode of particle detachment. Both these effects illustrated the relationship between shear and normal forces in the removal of rigid particles from deformable surfaces. The direct measure of fine particle removal forces

whilst observing their detachment should prove useful to the study of many applied processes.

Acknowledgements

This work was jointly sponsored by the Australian Research Council (ARC), the University of Wollongong and BHP Australia. The PDMS and the JKR measurements were made by Robert Oslanec, whose help is greatly appreciated.

References

[1] Eastman, T. and Zhu, D. M., *Langmuir* **12**(11), 2859 (1996).
[2] Lin, X. Y., Creuzet, F. and Arribart, H., *J. Phys. Chem.* **97**(28), 7272 (1993).
[3] Drummond, C. J. and Senden, T. J., *J. Colloids Surf.* **A87**, 217 (1994).
[4] Ducker, W. A., Senden, T. J. and Pashley, R. M., *Nature* **353**, 239 (1991).
[5] Toikka, G. and Hayes, R. A., *J. Colloid Interface Sci.* **191**, 102 (1997).
[6] Rabinovich, Y. I. and Yoon, R. H., *Langmuir* **10**(6), 1903 (1993).
[7] Toikka, G., Hayes, R. A. and Ralston, J., *J. Chem. Soc., Faraday Trans.* **93**(19), 3523 (1997).
[8] Larson, I., Drummond, C. J., Chan, D. Y. C. and Grieser, F., *J. Phys. Chem.* **99**(7), 2114 (1995).
[9] Toikka, G., Hayes, R. A. and Ralston, J., *Langmuir* **12**(16), 3783 (1996).
[10] Schaefer, D. M., Carpenter, M., Gady, B., Reifenberger, R., DeMejo, L. P. and Rimai, D. S., *J. Adhesion Sci. Technol.* **9**(8), 1049 (1995).
[11] Toikka, G., Hayes, R. A. and Ralston, J., *J. Colloid Interface Sci.* **180**, 329 (1996).
[12] Mizes, H. A., *J. Adhesion* **51**, 155 (1995).
[13] Biggs, S. and Spinks, G., *J. Adhesion Sci. Technol.* **12**(5), 461 (1998).
[14] DeMejo, L. P., Rimai, D. S. and Bowen, R. C., *Particles on Surfaces*, Mittal, K. L., Ed. (Plenum, New York, 1989), pp. 49–58.
[15] DeMejo, L. P., Rimai, D. S. and Bowen, R. C., *J. Adhesion Sci. Technol.* **5**(11), 959 (1991).
[16] DeMejo, L. P., Rimai, D. S., Chen, J. H. and Bowen, R. C., *Particles on Surfaces*, Mittal, K. L., Ed. (Marcel Dekker, Inc, New York, 1995), pp. 33–45.
[17] Bowen, R. C., DeMejo, L. P. and Rimai, D. S., *J. Adhesion* **51**, 201 (1995).
[18] Rimai, D. S., Moore, R. S., Bowen, R. C., Smith, V. K. and Woodgate, P. E., *J. Mater. Res.* **8**(3), 662 (1993).
[19] Rimai, D. S., DeMejo, L. P. and Bowen, R. C., *J. Adhesion* **51**, 139 (1995).
[20] Israelachvili, J. N. In: *Fundamentals of Friction: Microscopic and Macroscopic Processes*, Singer, I. L. and Pollock, H. M. Eds. (Kluwer, Dordrecht, 1992), pp. 351–385.
[21] Soltani, M. and Ahmadi, G., *J. Adhesion Sci. Technol.* **8**(7), 763 (1994).
[22] Toikka, G., Hayes, R. A. and Ralston, J., *J. Adhesion Sci. Technol.* **11**(12), 1479, (1997).
[23] Johnson, K. L., Kendall, K. and Roberts, A. D., *Proc. R. Soc. London, Ser.* **A324**, 301 (1971).
[24] Dupre, A., *Theorie Mechanique de La Chaleur* (Gauthier-Villars, Paris, 1869).
[25] Barquins, M., *J. Adhesion* **14**, 63 (1982).

[26] Rimai, D. S., DeMejo, L. P., Vreeland, W., Bowen, R. C., Gaboury, S. R. and Urban, M. W., *J. App Phys.* **71**(5), 2253 (1992).
[27] Kim, S., Choi, G. Y., Ulman, A. and Fleischer, C., *Langmuir* **13**, 6850 (1997).
[28] Perutz, S., Kramer, E. J., Baney, J. M. and Hui, C.-Y., *Macromolecules* **30**(25), 7964 (1997).
[29] Perutz, S., Kramer, E. J., Baney, J. M., Hui, C.-Y. and Cohen, C., *J. Polym. Sci. Part A: Polym. Chem.* **36**(12), 2129 (1998).
[30] Rimai, D. S., DeMejo, L. P., Vreeland, W. B. and Bowen, R. C., *Langmuir* **10**(11), 4361 (1994).
[31] Israelachvili, J. N., *Intermolecular and Surface Forces*, 2nd edn. (Academic Press, London, 1992).
[32] Barquins, M., *M. Mater. Sci. Eng.* **73**, 45 (1985).
[33] Maugis, D., *J. Colloid Interface Sci.* **150**(1), 243 (1992).
[34] Attard, P., *Langmuir* **15**(2), 553 (1999).